Electronic Supplementary Material (ESI) for Nanoscale Advances.

Supporting Information for: Impact of the Ga flux incidence angle on the growth kinetics of self-assisted GaAs nanowires on Si(111)

Marco Vettori,[†] Alexandre Danescu,[*,†] Xin Guan,[†,‡] Philippe Regreny,[†] José Penuelas,[†] and Michel Gendry[†]

[†]*Université de Lyon, Institut des Nanotechnologies de Lyon - INL, UMR CNRS 5270, Ecole Centrale de Lyon, 69134 Ecully, France*

[‡]*Physics Department, Lancaster University, Bailrigg, Lancashire LA1 4YW,UK*

E-mail: alexandre.danescu@ec-lyon.fr

Comparing samples grown at different incidence angles of the Ga flux

In order to determine the impact of the incidence angle of the Ga flux on the NW growth, samples were realized for comparison by employing either the Ga(5) or the Ga(7) cell and growing the NWs for the same time under identical experimental conditions, reported in the Experimental Section. SEM images of the corresponding samples are herein reported in Figure 1.

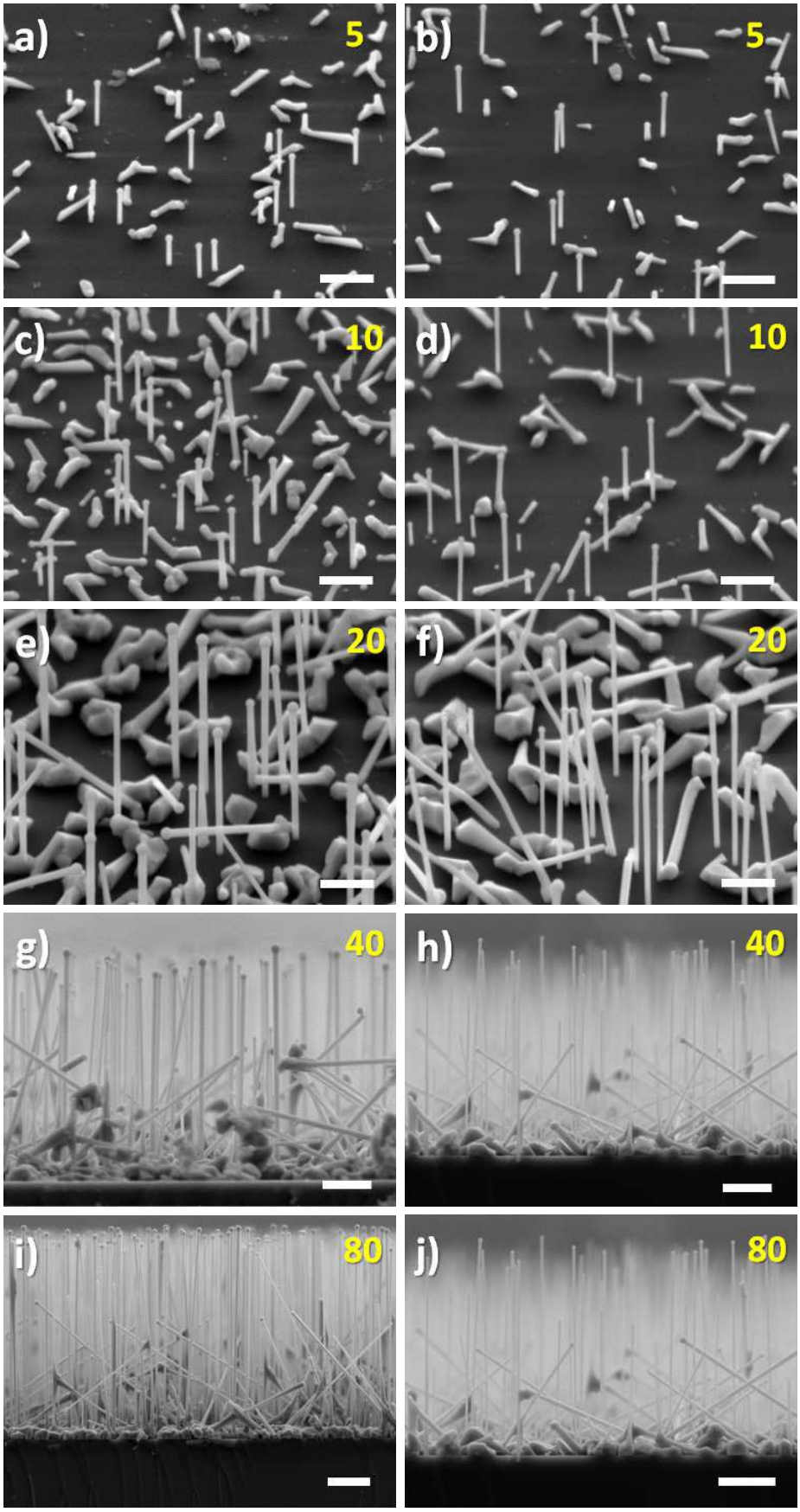

Figure 1: SEM images of Ga(5)As NWs (a, c, e, g, i) and Ga(7)As NWs (b, d, f, h, j) for increasing growth times. The growth time in min is indicated by the yellow numbers. The white scale bars correspond to 500 nm in (a, b, c, d, e, f) and to 2 μm in (g, h, i, j). SEM images in a, b, c, d, e, f are 45-tilted. SEM images in g, h, i, j are cross-section images.

Wetting angle and crystal structure

As already reported by other groups,[1,2] the wetting angle of the catalyst droplet can have a dramatic effect on the crystal structure of VLS-grown GaAs NWs. This is observed also in our case, suggesting an influence of the Ga flux incidence angle on the crystal structure. For example, TEM images of Ga(5)As and Ga(7)As NWs grown for 80 min (Figure 2) show that the Ga(5) source originates droplets with high wetting angle (137°) which determines a ZB crystal structure in the NW. On the other hand, the use of the Ga(7) source induces droplets with lower wetting angle (119°) leading to NWs with a Wz crystal structure. Such results suggest that it might be possible to tune the NW crystal structure by controlling the wetting angle of the Ga droplet through the incidence angle of the Ga flux.

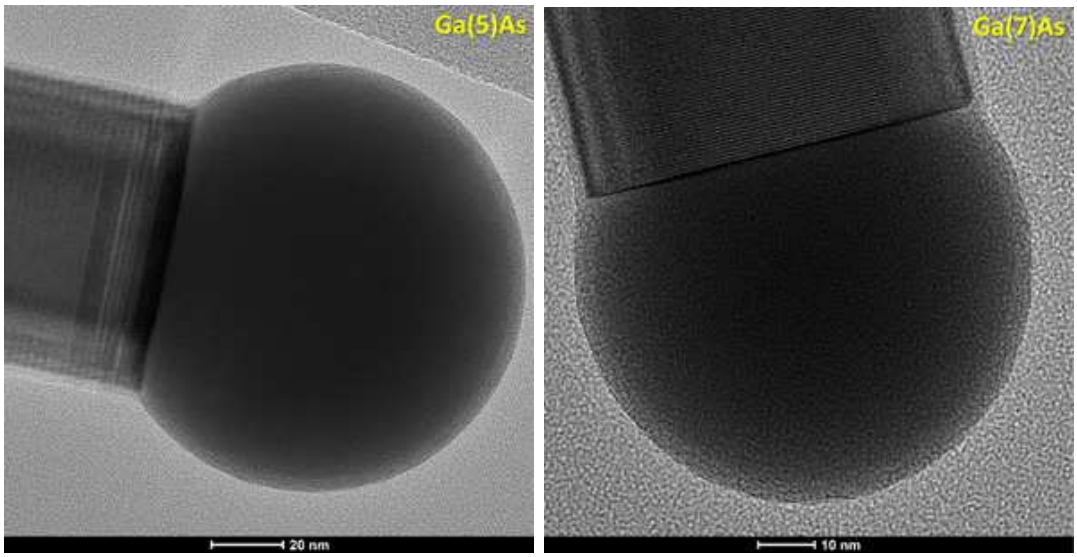

Figure 2: TEM images with [1$\bar{1}$0] zone axis of Ga(5)As and Ga(7)As NWs grown for 80 min, showing a Ga droplet with a wetting angle of 137° and a NW with a ZB structure (left) and a Ga droplet with a wetting angle of 119° and a NW with a Wz structure (right), respectively. The TEM images were recorded by G. Patriarche at C2N-CNRS, Palaiseau (France).

Nanowires grown for short times

Figure 3 shows SEM images of NWs obtained with Ga(5) or Ga(7) cell for growth times in the 20 sec - 3 min range under the same conditions reported in the experimental section.

The images were recorded at a grazing angle of 5°.

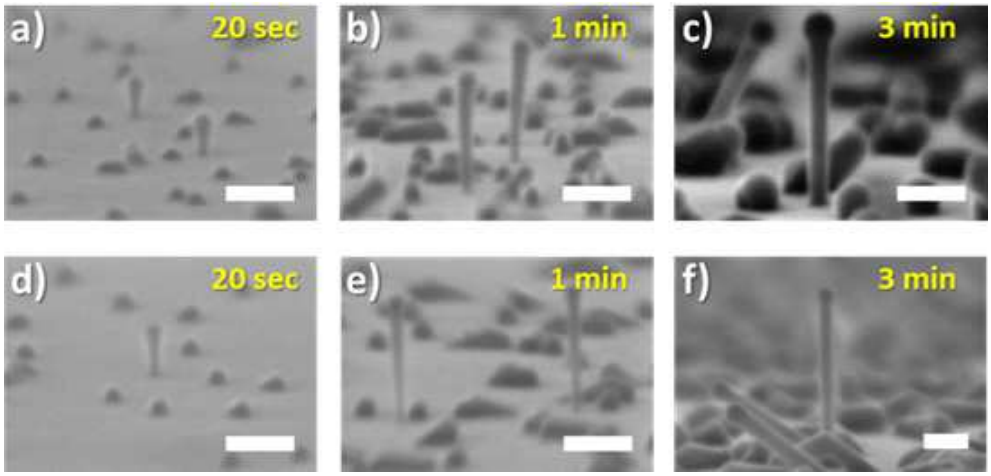

Figure 3: SEM grazing images (5°-tilted) of: (a-c) Ga(5)As NWs and (d-f) Ga(7)As NWs obtained for shorter growth times. The yellow captions correspond to the GaAs growth time. The white scale bars correspond to 100 nm.

Ga deposition and NW nucleation

In order to monitor all the steps of the growth procedure, so as to provide more precise empirical parameters to simulate the NW growth, we adopted the same growth conditions reported in the experimental section and prepared several samples to follow the growth in its early stages.

It can thus be observed that the pre-deposition of 1 ML of Ga at 520°C leads to the formation of droplets with diameter (D) equal to 16 ± 3 nm and density (d) of $\simeq 30$ μm^{-2} (Figure 4(a)), which is consistent with a usual range of d between 15 and 40 μm^{-2}, as measured on several samples.

While increasing the substrate temperature up to 610°C, the Ga droplets are expected to drill pinholes in the SiO_2 surface layer[3] by reducing SiO_2 and forming Ga_2O and SiO volatile compounds, which finally desorb.[4,5] This is confirmed by Figure 4(b), where no more Ga droplets are visible on the surface after such a procedure.

Samples were then realized after such a treatment by exposition to Ga and As fluxes for short growth times (2, 12 and 20 sec). It is thus possible to observe that after 2 sec

exposition (Figure 4(c, d)) the Ga droplets reform with $d \simeq 25\ \mu\text{m}^{-2}$ and $D = 22 \pm 3$ nm. After 12 sec exposition the system is substantially unchanged (Figure 4(e, f)), with Ga droplets presenting $d \simeq 40\ \mu\text{m}^{-2}$ and $D = 22 \pm 3$ nm. The situation changes significantly after 20 sec exposition: in fact, apart from the Ga droplets which show values of d and D comparable to the previous ones ($d \simeq 25\ \mu\text{m}^{-2}$ and 27 ± 4 nm, respectively), NWs finally appear (Figure 4(g, h)). These show $d \simeq 1.2\ \mu\text{m}^{-2}$, length $L = 58 \pm 4$ nm and $D = 15 \pm 4$ nm. The value of the NW diameter at the very beginning of the axial growth is particularly important, since it constitutes a parameter to be employed in our semi-empirical model to correctly simulate the NW growth kinetics.

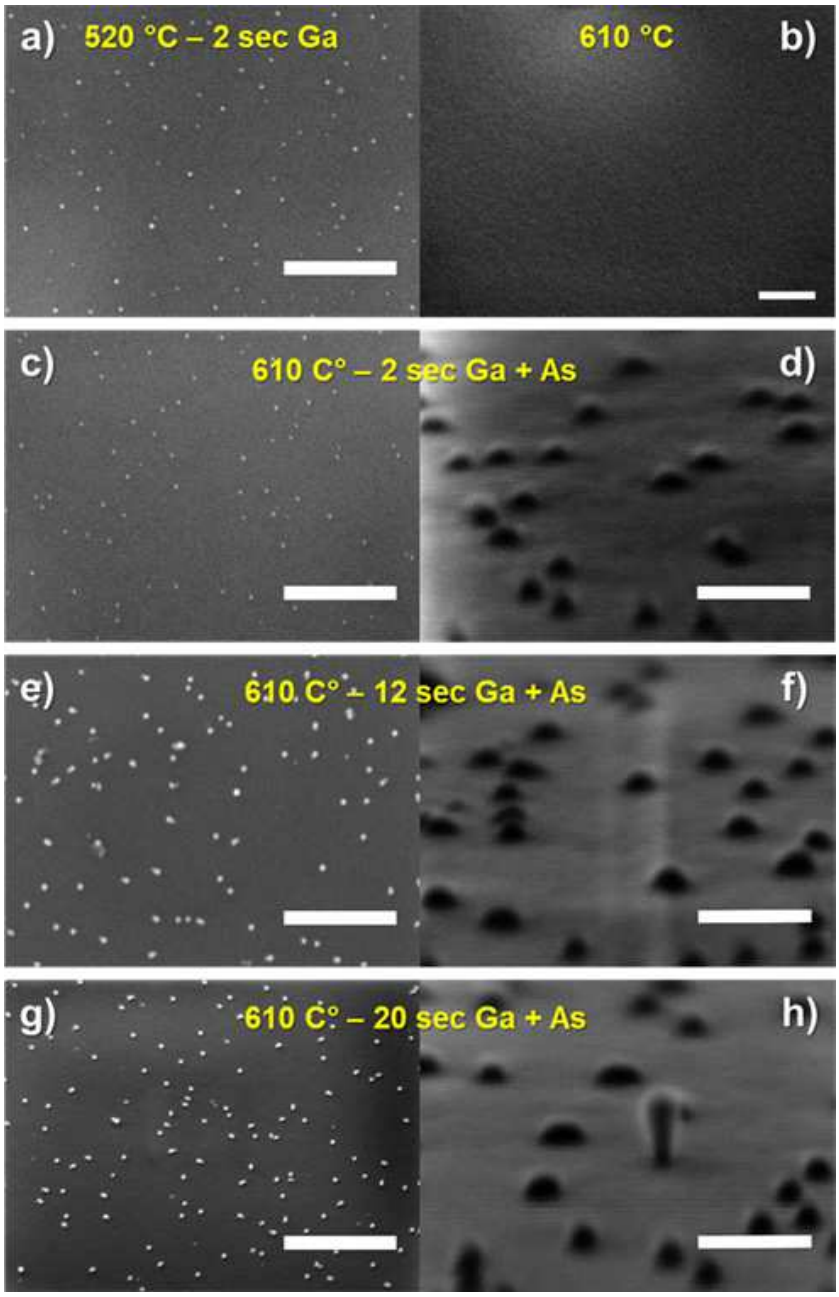

Figure 4: SEM images showing the early stages of the growth procedure employed. (a) Top-view of Ga droplets obtained after pre-deposition of 1 ML of Ga at 520°C. (b) Top-view of Ga-free surface after the temperature increasing to $T_{growth} = 610$°C. (c) Top-view and (d) grazing (5°-tilted) view of Ga droplets re-formed after 2 sec exposition to Ga and As fluxes. (e) Top-view and (f) grazing (5°-tilted) view after 12 sec exposition. (g) 45°-tilted view and (h) grazing (5°-tilted) view after 20 sec exposition. The values reported in yellow correspond to the temperature at which every step was performed. White scale bars correspond to 500 nm in (a, b, c, e, g) and to 100 nm in (d, f, h).

Implementation of the proposed model

We provide hereafter the algorithm we used for the numerical implementation of our model.

1. Fix the model parameters : λ_{SiO_2}, λ_{facet}, β_{min}, β_{max}, ϵ.
2. Provide experimental parameters : α_{As} α_{Ga}, F_{As}, F_{Ga}.
3. Initialize time $t = 0$ and fix the time step Δt.
4. Initialize $r(0)$, $V(0)$, $c(0)$ and $L(0)$.
5. Check if $\beta_{min} \leq \beta(0) \leq \beta_{max}$ and **Stop the algorithm** if not (initial conditions incompatible with the model parameters).
6. Loop over the time step :

   6.1 From $V(t)$ and $c(t)$; compute number of atoms $N_{As}(t)$ and $N_{Ga}(t)$ in the liquid phase.

   6.2 Compute q_{Ga}^{sub}, q_{Ga}^{facets} and $q_{Ga}^{droplet}$ from relations (1)-(3).

   6.3 Compute q_{As} from relation (4).

   6.4 Estimate $\hat{Q}_{Ga}(t)$, $\hat{Q}_{As}(t)$ and $\hat{c}(t)$ using relations (5)-(6).

   6.5 If $\hat{c}(t) \leq c^\star$ there is **no axial growth**. Update $r(t + \Delta t) = r(t)$ and :

      6.5.1 Compute the volume $\hat{V}(t)$ occupied by the quantities $\hat{Q}_{Ga}(t)$ and $\hat{Q}_{As}(t)$.

      6.5.2 If $\hat{V}(t)$ cannot be pinned at the top of a cylinder of radius $r(t)$ with an angle $\leq \beta_{max}$ then **Stop the algorithm** (the droplet is unstable). Otherwise :

         6.5.2.1 Update $V(t + \Delta t) = \hat{V}(t)$ and concentration $c(t + \Delta t) = \hat{c}(t)$. **Continue the loop over the time step** at step 6.

   6.6 If $\hat{c}(t) > c^\star$ **axial growth takes place** but we have to check if the radius of the NW will change or not. To do this :

   6.7 Compute $Q(t)$, the equal amount of Ga and As such that, for the remaining quantities the concentration is $c^\star$. This is exactly

$$Q(t) = \hat{Q}_{As}(t) \frac{1 - c^\star/\hat{c}}{1 - 2c^\star/\hat{c}} \tag{1}$$

6.8 Compute the solid volume $V_S(t)$ occupied by the total amount (of equal quantities) of Ga and As. **Stop the algorithm** if the remaining volume $V(t+\Delta t) = \hat{V}(t) - V_S(t)$ is too small. Otherwise :

6.8.1 If the remaining liquid volume $V(t+\Delta t)$ containing $\hat{Q}_{Ga}(t) - Q(t)$ and $\hat{Q}_{As}(t) - Q(t)$ (and has As concentration equal to $c^\star$) can be pinned at the top of the droplet with radius $r(t)$ and wetting angle in the interval $(\beta_{min}, \beta_{max})$, we have **axial growth at constant radius**; update $L(t+\Delta t) = L(t) + V_S/(\pi r^2(t))$, $c(t+\Delta t) = c^\star$ and $r(t+\Delta t) = r(t)$; **Continue the loop over the time step** at step 6.

6.8.2 If the remaining liquid volume $V(t+\Delta t)$ (containing $\hat{Q}_{Ga}(t) - Q(t)$ and $\hat{Q}_{As}(t) - Q(t)$) cannot be pinned at the top of the droplet with radius $r(t)$ since the wetting angle is $< \beta_{min}$, then **we have axial growth and direct tapering**; compute the unique value $r(t+\Delta t) < r(t)$ such that the liquid volume can be pinned at the top of the cylinder with radius $r(t+\Delta t)$ at wetting angle β_{min}. Then, the solid volume $V_S(t)$ computed at 6.8 will fill a truncated cone with lower radius $r(t)$ and upper radius $r(t+\Delta t)$. Update the length of the NW using

$$L(t+\Delta t) = L(t) + \frac{3V_S(t)}{\pi(r^2(t) + r(t)r(t+\Delta t) + r^2(t+\Delta t))}, \qquad (2)$$

$c(t+\Delta t) = c^\star$ and $r(t+\Delta t)$. **Continue the loop over the time step** at step 6.

6.8.3 If the remaining liquid volume $V(t+\Delta t)$ cannot be pinned at the top of the droplet with radius $r(t)$ since the wetting angle is $> \beta_{max}$, then we have **axial growth and inverse tapering**; compute the unique value $r(t+\Delta t) > r(t)$ such that the liquid volume can be pinned at the top of the cylinder with radius $r(t+\Delta t)$ at wetting angle β_{max}. Then the solid volume computed at 6.8 will fill a truncated cone with lower radius $r(t)$ and upper radius $r(t+\Delta t)$. Update the volume using formula (1) and

$c(t + \Delta t) = c^{\star}$ and $r(t + \Delta t)$. **Continue the loop over the time step** at step 6.

We remark here that the above algorithm is also able to simulate both time-dependent flux values and time-dependent alternating source positions, as well as multiple sources. As already noticed, the above algorithm represents an average situation when shadowing and re-emission effects are not explicit (but actually included in the definitions of average diffusion lengths introduced above).

References

(1) Jacobsson, D.; Panciera, F.; Tersoff, J.; Reuter, M. C.; Lehmann, S.; Hofmann, S.; Dick, K. A.; Ross, F. M. Interface dynamics and crystal phase switching in GaAs nanowires. *Nature* **2016**, *531*, 317.

(2) Harmand, J.-C.; Patriarche, G.; Glas, F.; Panciera, F.; Florea, I.; Maurice, J.-L.; Travers, L.; Ollivier, Y. Atomic step flow on a nanofacet. *Physical Review Letters* **2018**, *121*, 166101.

(3) Fontcuberta i Morral, A.; Colombo, C.; Abstreiter, G.; Arbiol, J.; Morante, J. Nucleation mechanism of gallium-assisted molecular beam epitaxy growth of gallium arsenide nanowires. *Applied Physics Letters* **2008**, *92*, 063112.

(4) Wright, S.; Kroemer, H. Reduction of oxides on silicon by heating in a gallium molecular beam at 800° C. *Applied Physics Letters* **1980**, *36*, 210–211.

(5) Madsen, M. H.; Aagesen, M.; Krogstrup, P.; Sørensen, C.; Nygård, J. Influence of the oxide layer for growth of self-assisted InAs nanowires on Si(111). *Nanoscale research letters* **2011**, *6*, 516.